ISSN 0006-2979, Biochemistry (Moscow), 2023, Vol. 88, No. 9, pp. 1356-1367 © Pleiades Publishing, Ltd., 2023.
Russian Text © The Author(s), 2023, published in Biokhimiya, 2023, Vol. 88, No. 9, pp. 1642-1654.

Production and Characterization of Photorin, a Novel Proteinaceous Protease Inhibitor from the Entomopathogenic Bacteria *Photorhabdus laumondii*

Igor M. Berdyshev[1#], Anastasia O. Svetlova[1#], Ksenia N. Chukhontseva[1], Maria A. Karaseva[1], Anna M. Varizhuk[2], Vasily V. Filatov[3], Sergey Y. Kleymenov[4,5], Sergey V. Kostrov[1], and Ilya V. Demidyuk[1,a]*

[1] *National Research Centre "Kurchatov Institute", 123182 Moscow, Russia*

[2] *Moscow Institute of Physics and Technology (National Research University), 141701 Dolgoprudny, Moscow Region, Russia*

[3] *Semenov Federal Research Center for Chemical Physics, Chernogolovka Branch, Russian Academy of Sciences, 142432 Chernogolovka, Moscow Region, Russia*

[4] *Bach Institute of Biochemistry, Research Center of Biotechnology, Russian Academy of Sciences, 119071 Moscow, Russia*

[5] *Koltzov Institute of Developmental Biology, Russian Academy of Sciences, 119334 Moscow, Russia*

[a] *e-mail: ilyaduk@yandex.ru*

Received April 13, 2023
Revised May 27, 2023
Accepted June 17, 2023

Abstract—Entomopathogenic bacteria of the genus *Photorhabdus* secrete protease S (PrtS), which is considered a virulence factor. We found that in the *Photorhabdus* genomes, immediately after the *prtS* genes, there are genes that encode small hypothetical proteins homologous to emfourin, a recently discovered protein inhibitor of metalloproteases. The gene of emfourin-like inhibitor from *Photorhabdus laumondii* subsp. *laumondii* TT01 was cloned and expressed in *Escherichia coli* cells. The recombinant protein, named photorin (Phin), was purified by metal-chelate affinity and gel permeation chromatography and characterized. It has been established that Phin is a monomer and inhibits activity of protealysin and thermolysin, which, similar to PrtS, belong to the M4 peptidase family. Inhibition constants were 1.0 ± 0.3 and 10 ± 2 μM, respectively. It was also demonstrated that Phin is able to suppress proteolytic activity of *P. laumondii* culture fluid (half-maximal inhibition concentration 3.9 ± 0.3 nM). Polyclonal antibodies to Phin were obtained, and it was shown by immunoblotting that *P. laumondii* cells produce Phin. Thus, the *prtS* genes in entomopathogenic bacteria of the genus *Photorhabdus* are colocalized with the genes of emfourin-like inhibitors, which probably regulate activity of the enzyme during infection. Strict regulation of the activity of proteolytic enzymes is essential for functioning of all living systems. At the same time, the principles of regulation of protease activity by protein inhibitors remain poorly understood. Bacterial protease-inhibitor pairs, such as the PrtS and Phin pair, are promising models for *in vivo* studies of these principles. Bacteria of the genus *Photorhabdus* have a complex life cycle with multiple hosts, being both nematode symbionts and powerful insect pathogens. This provides a unique opportunity to use the PrtS and Phin pair as a model for studying the principles of protease activity regulation by proteinaceous inhibitors in the context of bacterial interactions with different types of hosts.

DOI: 10.1134/S0006297923090158

Keywords: proteinaceous protease inhibitor, *Photorhabdus*, entomopathogenic bacteria, protealysin, emfourin, photorin

Abbreviations: Abz-RSVIK(Dnp), 2-aminobenzoyl-L-arginyl-L-seryl-L-valyl-L-isoleucyl-L-(ε-2,4-dinitrophenyl)lysine; CD, circular dichroism; DSC, differential scanning calorimetry; ELI, emfourin-like inhibitor; GPC, gel permeation chromatography; MCAC, metal-chelate affinity chromatography; M4in, emfourin; PLP, protealysin-like protease; Phin, photorin; Pln, protealysin; PrtS, protease S; PPI, proteinaceous protease inhibitor; Tln, thermolysin; TT01, *Photorhabdus laumondii* subsp. *laumondii* TT01.

* To whom correspondence should be addressed.
# These authors contributed equally to this study.

INTRODUCTION

Proteolytic enzymes play a vital role in functioning of all live systems. Activity of proteases is under strict control, which ensures high selectivity of their action and prevents aberrant proteolysis. One of the factors regulating activity of proteolytic enzymes are endogenous selective proteinaceous protease inhibitors (PPIs). Functions of PPIs have been elucidated in detail in some important cases [1-5], however, general principles of regulation of protease activities by PPIs in live systems remain poorly understood.

Bacterial protease–inhibitor pairs are in our opinion very promising models for investigation of the principles of *in vivo* regulation by proteinaceous inhibitors. Main advantage of the suggested model is wide availability of biological systems, their lower complexity, and convenience from the experimental point of view. Furthermore, existence of a large number of orthologous protease–inhibitor pairs in bacteria from different taxa allows considering regulation from the evolutionary perspective. However, very little is known about the bacterial PPIs in comparison with the eukaryotic ones. In particular, the database of peptidases and their proteinaceous inhibitors MEROPS (www.ebi.ac.uk/merops/) [6] currently includes 18,000 sequences of bacterial origin and more than 155,000 sequences of eukaryotic PPIs (as of March 22, 2023). Natural targets and biological functions have not been elucidated for the majority of bacterial PPIs. At the same time, in some cases establishing of functional connections between bacterial proteases and their inhibitors could be achieved based on localization of their genes in the same operon [7].

Recently we have discovered a new family of proteinaceous inhibitors of metalloproteases, family I104 in the MEROPS database (www.ebi.ac.uk/merops/cgi-bin/famsum?family=I104), and characterized a prototype of the family, emfourin (M4in) from *Serratia proteamaculans*. Genes of the emfourin-like inhibitors (ELIs) in bacteria and archaea are co-localized with the genes of homologues of protealysin (Pln) from *S. proteamaculans* [8, 9], protealysin-like proteases (PLP) from the peptidase family M4 (www.ebi.ac.uk/merops/cgi-bin/famsum?family=M4). In *S. proteamaculans* the genes of ELI and PLP form a bicistronic operon, however, in many other bacterial species these are, likely, two independent genes, but located one after another. It has been demonstrated for M4in that it strongly inhibits Pln. Hence, it is likely that PLPs are natural targets of ELIs, and that these proteins probably are associated with common biological functions [7].

Biological role of ELIs and PLPs is poorly understood. However, there are data available indicating participation of PLPs in penetration of bacteria into human cells [10-14], suppression of immune system of insects [15, 16] and fish [17], as well as destruction of the proteins in plant cell wall [18, 19]. Moreover, it has been suggested that ELI and PLP are elements of an unidentified system of interbacterial competition [7, 20]. Hence, PLPs are probably multifunctional proteins involved in the interaction of bacteria with higher organisms and, in particular, in pathogenesis, as well as in interactions of bacteria between themselves, while ELIs control activity of PLPs in all mentioned situations. Based on this it is only logical to suggest that the ELI–PLP pair could serve as a model for investigation of principles of regulation of proteolytic activity by proteinaceous inhibitors. Success of such studies would obviously significantly depend on the selection of the model organism.

Entomopathogenic bacteria of the *Photorhabdus* genus seem to be most promising in this regard. The most investigated representative of this genus is *Photorhabdus laumondii* subsp. *laumondii* TT01 (TT01) (formerly known as *Photorhabdus luminescens* subsp. *laumondii* TT01). These bacteria have a complex lifecycle acting either as symbionts of nematodes from the Heterorhabditidiae family, or as strong insect pathogens, which provides a unique opportunity to investigate various types of interactions of bacteria with their hosts [21]. It should be mentioned in the context of our discussion that the *Photorhabdus* cells invade the cells of rectal gland in nematodes [22] and manipulate immune system of the infected insects [21]. Moreover, bacteria of the *Photorhabdus* genus exhibit antibacterial and antifungal activity [23, 24]. PLPs from several *Photorhabdus* strains (proteases S, PrtS) have been characterized to a varying degree [15, 16, 25, 26].

The published data allow concluding that PrtS is likely not the main insectotoxin in the bacteria, but, at the same time, it likely participates in interaction of bacteria with the insect immune system affecting antibacterial peptides and inducing melanization process [15, 16]. However, these data are fragmentary, and biological functions of PrtS, as well as other PLPs, should be investigated further. Many assumed functions of PLPs presumably are realized in *Photorhabdus*, and this model seems to be promising for investigation of these enzymes. In particular, it could be used for investigation of regulation of activity of PLPs with the help of ELIs. However, currently there are no data on ELIs in the bacteria of the *Photorhabdus* genus.

In the *Photorhabdus* genomes the genes encoding hypothetical proteins homologous to M4in are located immediately after the *prtS* genes. In this study one of these genes (from TT01) was for the first time cloned and expressed in the *Escherichia coli* cells. The recombinant protein, named photorin (Phin), was purified and characterized. It was shown that Phin inhibits PLPs and is produced by the TT01 cells. The obtained data indicate that the ELI–PLP pair is functional in the bacteria of *Photorhabdus* genus, and that these bacteria could be used as a model to investigate principles of regulation of protease activity by proteinaceous inhibitors.

Table 1. Primers used

Primer name	Sequence
EcoRI_D1	TCAAGAATTCGCAAAAAACTGGATATGATTTTCCATC
TT01_R1	TCATTGAACGAATCCCTAC
TT01_D2	GTAGGGATTCGTTCAATGA
HindIII_R2	CTCGAAGCTTTAATCCGCCAATTGTTGTGATCCACG
HindIII_R3	ACTCAAGCTTCCGGATCTGCATCGCAGGATG
EcoRI_D3	ATGAGAATTCTTGAAGACGAAAGGGGGCCTCGT
FauNDI_D4	GGAACATATGAATAATAAAACGCTCAA
XhoI_R4	GAATCTCGAGTTA**ATGGTGATGGTGATGGTG**ACCACCCTTTTTGTCGGT

Note. Restriction sites of *Eco*RI, *Hind*III, *Fau*NDI, and *Xho*I are underlined. Site mediating introduction of an additional sequence encoding six histidine residues prior to the stop codon in the *phin* gene is shown in bold.

MATERIALS AND METHODS

General techniques. Protein concentration was determined using a modified Bradford assay with IgG as a standard [27, 28].

Concentration of purified proteins in solution was determined from absorption at 280 nm using extinction coefficients calculated with the help of the ProtParam service (https://web.expasy.org/protparam/): ε_{280} = = 52,370 $M^{-1}\cdot cm^{-1}$ – for Pln, ε_{280} = 58,200 $M^{-1}\cdot cm^{-1}$ – for thermolysin (Tln), and ε_{280} = 11,460 $M^{-1}\cdot cm^{-1}$ – for Phin.

Proteins were analyzed with electrophoresis in a 15% polyacrylamide gel containing 0.1% sodium dodecyl sulfate according to Laemmli [29]. Protein bands were stained with Coomassie Brilliant Blue G-250 (Reanal, Hungary). Precision Plus Protein Unstained Standards (Bio-Rad, USA) were used as molecular weight markers.

Transformation of *E. coli* cells with a DNA plasmid was carried out as described previously [30]. An *E. coli* TG1 strain was used for production of plasmids. DNA was purified with the help of Plasmid Miniprep or Cleanup Standard reagent kits (Evrogen, Russia).

Gel permeating chromatography was performed on a Superdex 75 10/300 GL column (GE Healthcare, Sweden). Column was calibrated with the help of a Gel Filtration Markers Kit for Protein Molecular Weights 6500-66,000 Da (Sigma-Aldrich, USA).

Sequencing of the produced genetic constructs as well as synthesis of all used oligonucleotides was performed in the Evrogen company.

Cloning of the photorin gene and construction of expression vector. Strain *P. laumondii* subsp. *laumondii* TT01 (TT01) was obtained from the German Collection of Microorganisms and Cell Cultures (strain DSM 15139, access number in RefSeq NC_005126.1). TT01 cells were cultivated overnight with aeration at 30°C in Lennox LB [31]. Cells from 1 ml of the bacterial suspension were precipitated with centrifugation (4000*g*, 10 min), re-suspended in 100 µl of deionized water, heated at 95°C for 10 min, and centrifuged (13,000*g*, 10 min). Supernatant (1 µl) was used for PCR with Pfu DNA polymerase (SibEnzyme, Russia) and pairs of oligonucleotide primers EcoRI_D1 and TT01_R1 or TT01_D2 and HindIII_R2 (Table 1). PCR products after purification were used together with primers EcoRI_D1 and HindIII_R2 for overlap extension PCR. The obtained fragments of the TT01 genome containing genes *prtS* (PLU_RS06905) and *phin* (PLU_RS06900), as well as flanking regions were purified, treated with restrictases EcoRI and HindIII (New England Biolabs, USA), and used for cloning. Fragment of the pBR322 plasmid was used as a cloning vector, which was amplified with the use of HindIII_R3 and EcoRI_D3 primers (Table 1), purified, cleaved with the same enzymes, and ligated using a Quick-TA T4 DNA ligase (Evrogen) with the fragment of the TT01 genome mentioned above. The obtained plasmid was named pTT01.

In order to construct expression plasmid pET-Phin, *phin* gene was amplified using pTT01 as a template and primers FauNDI_D4 and XhoI_R4 (Table 1). For cloning, the sites *Fau*NDI and *Xho*I were inserted into the primers. In addition, a site was inserted into the XhoI_R4 primer that mediated introduction of an additional sequence that encoded six histidine residues in front of the *phin* gene stop codon (shown in bold in the primer sequence, Table 1). PCR products were purified, treated with restrictases FauNDI (SibEnzyme) and XhoI (New England Biolabs), and ligated with the pET-23a vector cleaved with the same enzymes.

Structures of all cloned fragments were confirmed by sequencing.

Preparation of photorin. *E. coli* BL21 (DE3) cells (Novagen, USA) transformed with the pET-Phin plasmid were cultivated with shaking in 250 ml of a medium containing (per 1 liter) Na_2HPO_4 – 7.1 g, KH_2PO_4 – 6.8 g, $(NH_4)_2SO_4$ – 3.3 g, $MgCl_2 \times 6H_2O$ – 3.3 g, glycerol – 5 g, peptone – 10 g, yeast extract – 5 g, glucose – 25 g, lactose – 50 g, and ampicillin – 100 mg at 37°C for 3 h, and next at 16°C for 72 h. Cells were precipitated with centrifugation (4000*g*, 4°C, 10 min), resuspended in 25 ml of 50 mM Tris-HCl (pH 8.0), and treated with ultrasound at 4°C two times over 5 min (1-s pulse and 2-s pause). Cell lysate was centrifuged (9000*g*, 4°C, 10 min), and supernatant was loaded onto a column with 1 ml of a Nickel XPure Agarose Resin (UBPBio, USA) equilibrated with 50 mM Tris-HCl (pH 8.0). Column was first washed with the same buffer and next Phin was eluted with a linear imidazole concentration gradient (0-250 mM) in the same buffer. Fractions containing Phin (as determined from the results of electrophoretic analysis) were combined and concentrated using a Vivaspin Turbo 15 ultrafiltration device with 5 kDa MWCO (Sartorius, Germany). The obtained sample was loaded onto a Superdex 75 10/300 GL column equilibrated with 50 mM Tris-HCl (pH 7.4) containing 150 mM NaCl followed by elution with the same buffer with flow rate 0.5 ml/min. Fractions containing highest amount of Phin (determined with electrophoretic analysis) were combined and dialyzed twice (6 and 16 h) against 100 volumes of 50 mM NH_4HCO_3 using a SnakeSkin dialysis tubing with 3.5 kDa MWCO (Thermo Fisher Scientific, USA) at 4°C. After dialysis the Phin solution was centrifuged (8600*g*, 4°C, 15 min), and supernatant was lyophilized.

Mass-spectrometry analysis. Lyophilized preparation of purified Phin was dissolved at concentration 5 μM in a water/methanol/formic acid mixture [50/49.5/0.5 (*v/v*)]. Mass-spectrometry analysis was carried out with an Exactive Orbitrap instrument (Thermo Fisher Scientific) equipped with a special ion source [32]. The protein molecular mass was calculated from the array of peaks corresponding to multiply-protonated protein molecules in the obtained electrospray ionization mass spectra.

Differential scanning calorimetry (DSC). Measurements were carried out at Phin concentration 4.2 mg/ml with a MicroCal VP-Capillary DSC (Malvern Instruments, USA). DSC experiments and data processing were conducted as described previously [7].

Circular dichroism spectroscopy (CD). CD spectra were recorded with a Chirascan VX spectrophotometer (Applied Photophysics, United Kingdom) at room temperature with optical path length 0.05 cm. Phin was dissolved at concentration 0.15 mg/ml in a 10 mM Tris-HCl buffer (pH 7.4), centrifuged at 8600*g* and 4°C for 5 min, and spectrum of a supernatant was recorded. Spectra were analyzed with the help of DichroWeb program using CDSSTR method and standard data set 4 [33]. Standard deviation values for each structural type were calculated only for the DichroWeb predictions with total sum of the secondary structure fractions of 100%. PDBMD2CD web server was used for predicting CD spectra and calculation of the fractions of secondary structures based on 3D structures [34].

Immunoblotting. Electrophoretically homogenous preparation of Phin was used in the NPO BioTest Sistemy (Russia) for immunization of rabbits using a standard protocol. The obtained antiserum was used for conducting immunoblotting according to the technique described previously [35]. Purified Phin was used to test specificity of the obtained antibodies.

For analysis, TT01 were cultivated for 48 h with aeration at 30°C in Lennox LB [31]. Aliquots (100 μl) of bacterial suspension were taken 16, 24, 30, and 48 h after the start of cultivation. Cells were precipitated by centrifugation (6000*g*, 10 min) and re-suspended in 100 μl of a buffer containing 125 mM Tris-HCl buffer (pH 6.8), 2% SDS, 5% β-mercaptoethanol, 2 mM 1,10-phenanthroline, 0.01% bromophenol blue, and 20% glycerol. Supernatant (culture fluid) was treated with 100 μl of 50% TCA, centrifuged (10,000*g*, 10 min), precipitate was washed with acetone to remove TCA, and 100 μl of the same buffer was added to it. The samples of cells and culture fluid were incubated for 5 min at 95°C. Following incubation, the samples were diluted with the same buffer based on the differences of optical density of the initial bacterial suspension, so that 15 μl of the obtained solution (amount used for electrophoretic analysis) contain material corresponding to 100 μl of bacterial suspension with optical density of 1 unit. Proteins were separated with the help of SDS-electrophoresis in a 16% polyacrylamide gel using Tris-Tricine buffer system [36].

Determination of protealysin and thermolysin inhibition constants by photorin. Analysis of inhibitory effect of Phin on Pln and Tln was carried out using an internally quenched fluorescent peptide substrate 2-aminobenzoyl-L-arginyl-L-seryl-L-valyl-L-isoleucyl-L-(ε-2,4-dinitrophenyl)lysine (Abz-RSVIK(Dnp)) (Peptide 2.0, USA) [37] as described previously [38]. Fluorescence (excitation wavelength – 320 nm; emission wavelength – 420 nm) was recorded with a CLARIOstar Plus multi-mode microplate reader (BMG LABTECH, Germany). Reaction was carried out in a 50 mM Tris-HCl buffer (pH 7.4). Concentrations of Pln and Tln in the reaction mixture were 50 pM, of Abz-RSVIK(Dnp) – 30 or 90 μM. Phin concentrations in the case of Pln were 0.5, 1, 2, 4, 6, and 8 μM, and in the case of Tln – 1, 5, 10, 20, 30, and 40 μM. Three independent measurements were obtained for each experimental condition.

In the case of slow binding of inhibitor with the enzyme, kinetic curves were approximated with the

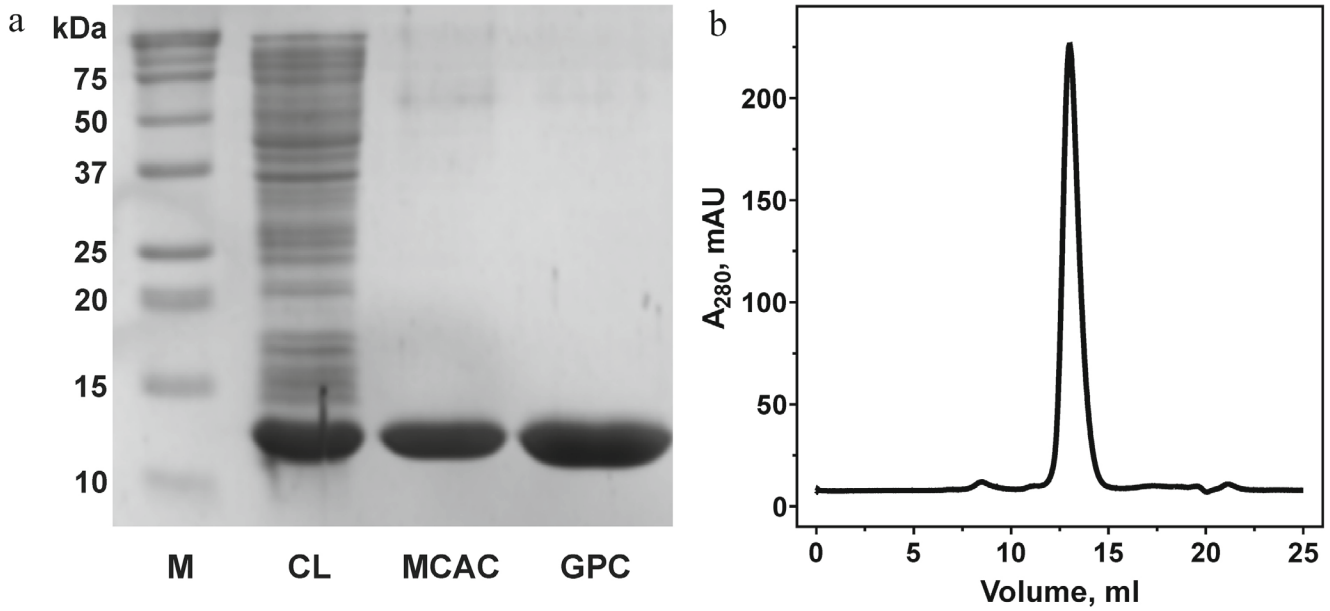

Fig. 1. Purification of recombinant photorin (Phin) and analysis of the purified protein. a) Electrophoretic analysis of Phin preparation at different purification steps; b) analysis of purified Phin with the help of gel permeation chromatography on a Superdex 75 10/300 GL column. M, Molecular mass standards; CL, supernatant of cell lysate; MCAC and GPC, samples after metal-chelate affinity chromatography and gel permeation chromatography, respectively.

integrated rate equation, and inhibition constants were calculated as described previously [39]. Inhibition constants K_i both for Pln and Tln were obtained using the Dixon method [40, 41]. Isomerization constant K_i^* for Pln was calculated in two steps using equations (1) and (2):

$$k_a = k_{-4} + \frac{k_{+4}[I]}{K_i\,(1 + [S] / K_M) + [I]}, \quad (1)$$

$$K_i^* = K_i \frac{k_{-4}}{(k_{+4} - k_{-4})}, \quad (2)$$

Calculations for Pln were performed using Michaelis constant K_M = 35 μM [37]. Data analysis was carried out with the help of GraphPad Prism version 8.0 program (GraphPad Software, USA).

Inhibition of activity of the *P. laumondii* subsp. *laumondii* TT01 culture fluid by photorin. TT01 cells were cultivated for 24 h with aeration at 30°C in Lennox LB [31]. Cells were precipitated by centrifugation at 4000*g* for 10 min. Supernatant was diluted 1000-fold with 50 mM Tris-HCl buffer (pH 7.4), and 10 μl of the obtained solution were used for measuring activity as described above for Pln and Tln. Concentration of Abz-RSVIK(Dnp) in the reaction mixture was 30 μM, Phin concentrations – 1, 2.5, 5, 7.5, and 10 nM. Rate of the substrate hydrolysis in the presence of inhibitor was determined from the linear region of the kinetic curves corresponding to the range 150-300 s after the start of fluorescence recording. IC_{50} was calculated using non-linear regression with the help of GraphPad Prism program.

RESULTS

Preparation of photorin. Gene of the putative emfourin-like inhibitor from the *P. laumondii* subsp. *laumondii* TT01 genome was cloned, modified to introduce a His_6-sequence at the protein C-terminus, and expressed in *E. coli* cells. The recombinant protein named photorin (Phin) was purified to electrophoretic homogeneity with the help of metal-chelate affinity chromatography (MCAC) and gel permeation chromatography (GPC); purification progress is presented in Fig. 1a and Table 2.

Average molecular mass of the purified Phin determined experimentally using mass spectrometry (12,517.1 Da) is in good agreement with the theoretical

Table 2. Recombinant photorin (Phin) purification

Purification step[a]	Total protein (mg)	Phin content (%)[b]	Yield (%)	Purification rate
Cell lysate	138	38	100	1.0
MCAC	48	86	80	2.3
GPC	10	98	20	2.6

[a]) MCAC – metal-chelate affinity chromatography; GPC, gel permeation chromatography.

[b]) Phin content was estimated with help of densitometry of protein bands in electrophoresis gels stained with Coomassie Brilliant Blue G-250.

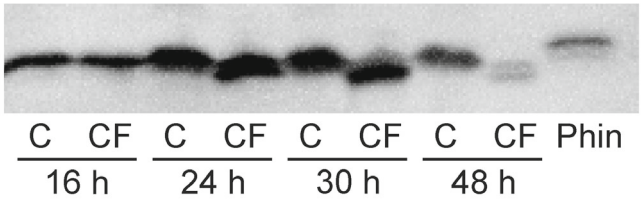

Fig. 2. Analysis of accumulation of photorin in the cells and culture fluid of *P. laumondii* subsp. *laumondii* TT01 using immunoblotting. C, cells TT01; CF, culture fluid; Phin, recombinant Phin (0.5 ng).

molecular mass of the protein (12,517.81 Da) calculated based on the protein sequence deduced from the gene and including N-terminal methionine and C-terminal His_6-sequence.

Based on the results of GPC analysis, molecular mass of the purified Phin was around 15.4 kDa (Fig. 1b). This value is slightly higher than the calculated mass likely due to the structural features of the protein. At the same time this result indicates that the main form of Phin in solution is a monomer.

Photorin is present in the cell and culture fluid of *P. laumondii*. It was demonstrated with the help of immunoblotting using rabbit polyclonal antibodies against Phin that Phin is accumulated in the cell and culture fluid of TT01 during batch cultivation (Fig. 2). Amount of the detected protein changes in the course of cultivation. Maximum amount of Phin was detected 24-30 h after inoculation, which corresponds to the beginning of the stationary phase of bacteria growth. In the late stationary phase (48 h) amount of Phin decreases significantly, which likely is associated with regulation of the *phin* gene activity with participation of Quorum Sensing.

Unexpectedly it was found that the inhibitor is detected in the cells and in the culture fluid of *P. laumondii* in approximately equal amounts. Intracellular localization of M4in was previously demonstrated, which correlates with the absence of known sorting signals in the ELI sequences (including the Phin sequence) [7]. It is likely that the release of Phin from the cells is non-specific and is due to the features of TT01. Furthermore, immunoblotting results demonstrate that after the end of logarithmic growth phase (24, 36, and 48 h) protein detected outside the cells has lower molecular mass than that of the intracellular protein. Moreover, there is much more significant decrease of the content of extracellular Phin in the late stationary phase than of the intracellular. This could indicate instability of Phin in the extracellular medium, but, at the same time, could be associated of unknown regulatory systems. One way or another, the obtained data imply that the issue on cellular localization of ELI remains unclear. This, however, does not affect the main conclusion from the described experiment: *phin* gene is expressed in the cells of the *P. laumondii* subsp. *laumondii* TT01, a natural producer of the inhibitor.

Photorin secondary structure. Secondary structure of Phin was evaluated with the help of CD spectroscopy. Analysis of the spectrum (Fig. 3) showed that relative contributions of α-helices, β-sheets, turns, and regions without regular secondary structures were 14 ± 5, 34 ± 2, 23 ± 3, and 30 ± 2%, respectively. The corresponding values calculated from the 3D structure of M4in [42, 43], prototype of the I104 inhibitor family to which Phin belongs, are 32 ± 3, 23 ± 9, 19 ± 5, and 27 ± 3%.

Hence, secondary structures of Phin and M4in differ significantly, which is unsurprising considering significant differences in the protein sequences (25% identity and 47% similarity). At the same time, despite of the almost 2-fold difference in the fraction of α-helices,

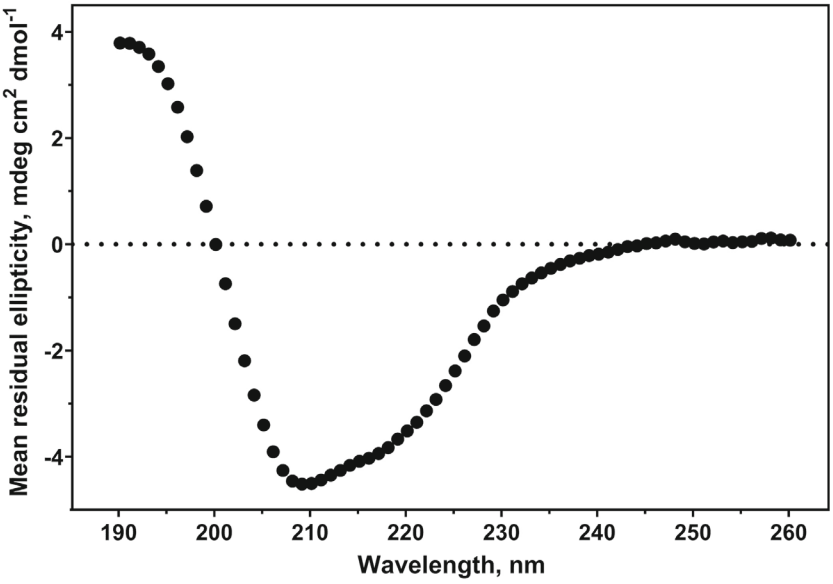

Fig. 3. CD spectrum of photorin.

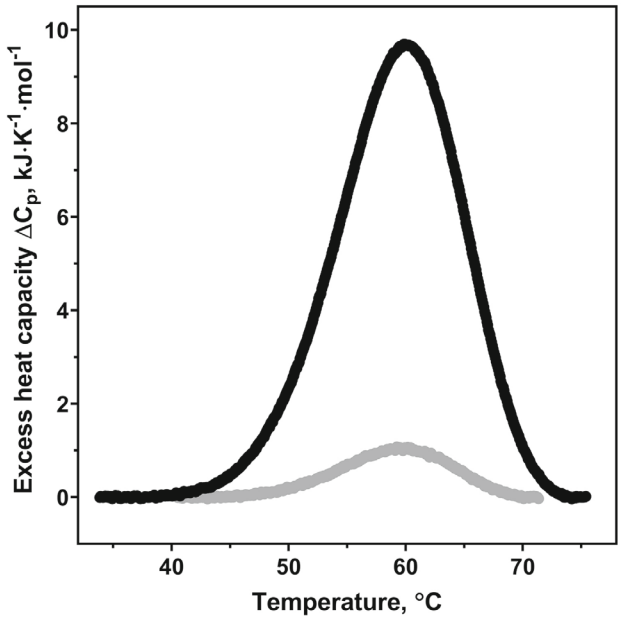

Fig. 4. Differential scanning calorimetry thermogram of photorin. Black and gray curves represent first and second round of heating, respectively.

both molecules are characterized with high fractions of α- and β-structures. These indicates that both these proteins belong to the same structural class α + β and could have common type of folding.

Thermostability of photorin. Thermal denaturation of Phin was investigated using the DSC method (Fig. 4). Phin demonstrated one thermal transition with maximum (T_{max}) at 60.2°C. Total calorimetric enthalpy (ΔH_{cal}) for Phin was 130.7 kJ/mol. Thermal denaturation of Phin was almost completely irreversible, because the second heating of the sample revealed ΔH_{cal} = 12.2 kJ/mol, which corresponded to only 9% of the initial calorimetric enthalpy. The third and fourth heating resulted in the decrease of enthalpy to 6% and 5% of the initial value, which corresponded to the standard drop of enthalpy of the reversible thermal denaturation with every subsequent heating.

Thermostability of Phin is close to thermostability of M4in, prototype of the I104 family, for which T_{max} = 61.2°C. However, unlike in the case of Phin, denaturation of M4in is completely irreversible, demonstrates three thermal transitions, and is characterized with ΔH_{cal} = 62.8 kJ/mol [7].

Denaturation enthalpy is determined by the total number of non-covalent interactions that stabilize a protein globule [44]. Increase of enthalpy in the case of Phin could be explained by the lower, in comparison with M4in, fraction of the regions with non-regular secondary structure and presence of more tightly packed regions, where stronger stabilizing interactions could be realized. Moreover, T_{max} is determined not only by the number of bonds, but also by their strength, localization, and other factors. Hence, the results of DSC, as well as the results of CD spectroscopy, indicate significant structural differences between Phin and M4in, which, at the same time, do not result in the significant differences in their thermostability.

Photorin inhibits protealysin and thermolysin through different mechanisms. Inhibitory activity of Phin against Pln and Tln was investigated. Kinetic curves obtained for inhibition of Pln by Phin had the shape characteristic for the slow-binding inhibitors and corresponded to the integrated rate equation [39] for this type of inhibition (in all cases R^2 was above 0.98). Values of the initial reaction rate (v_0) and apparent first-order rate constant (k_a) obtained using non-linear regression were used for constructing diagnostic diagrams (Fig. 5, Pln + Phin). Hyperbolic character of the dependencies of v_0 and k_a on Phin concentration indicates two-step mechanism [equation (3)], in which the rapidly formed initial enzyme–inhibitor complex (EI) is subjected to slow conformational transitions into the isomerized complex EI*:

$$E + I \underset{k_{-3}}{\overset{k_{+3}}{\rightleftharpoons}} EI \underset{k_{-4}}{\overset{k_{+4}}{\rightleftharpoons}} EI^*. \quad (3)$$

Based on this, equilibrium inhibition constant ($K_i = k_{-3}/k_{+3}$) was determined from the set of obtained v_0 values using Dixon method. To calculate rate constants k_{-4} and k_{+4}, the dependence of k_a on Phin was approximated with the equation (1) (Fig. 5, Pln + Phin). Equilibrium isomerization constant (K_i^*) was calculated using equation (2). The obtained constant values are presented in Table 3.

In general, conformational changes during interaction of an inhibitor with the enzyme could occur either before the initial contact of these molecules (conformational selection) or after (induced-fit) [45, 46]. The two-step mechanism described by the equation (3) and characteristic for the interaction between Phin and Pln represents the simplest case, when inhibitor binding occurs fast in comparison with the following conformational changes. This mechanism is realized under

Table 3. Inhibition constants of protealysin (Pln) and thermolysin (Tln) by photorin (Phin)[a]

Constants for Phin	Pln	Tln
K_i (μM)	1.0 ± 0.3	10.2 ± 1.9
k_{-4} (10^{-4}·s^{-1})	3.5 ± 0.6	n/a
k_{+4} (10^{-3}·s^{-1})	2.0 ± 0.4	n/a
K_i^* (nM)	153 ± 46	n/a

Note. [a] Values are presented as a mean ± standard error; n/a – not applicable.

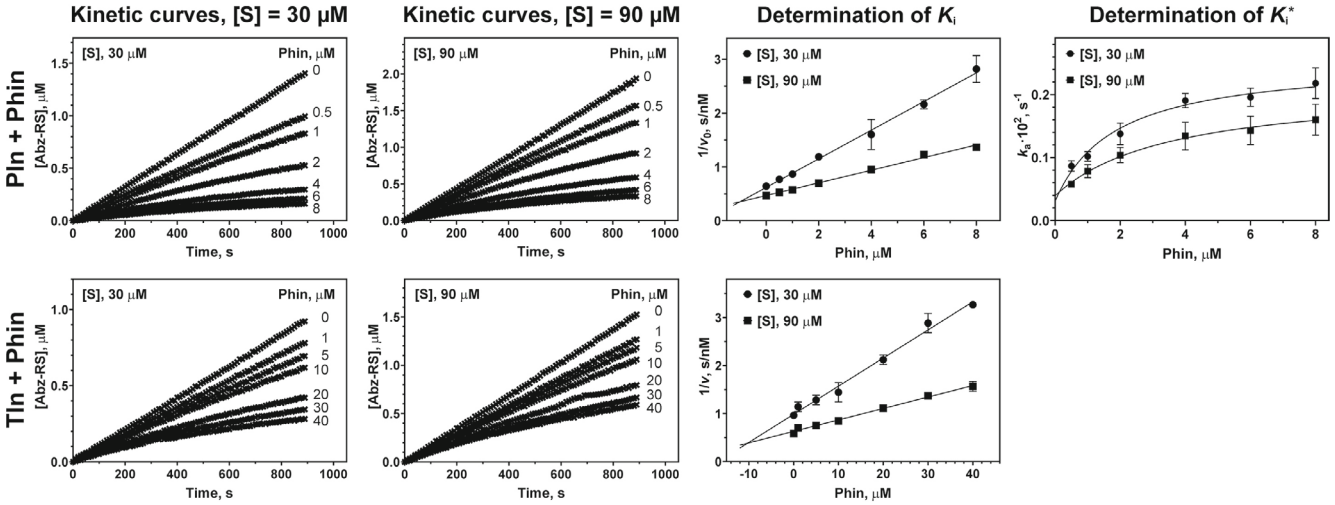

Fig. 5. Kinetic curves of the hydrolysis of Abz-RSVIK(Dnp) substrate by protealysin (Pln) and thermolysin (Tln) in the presence of photorin (Phin) and determination of inhibition constants. Kinetic curves were obtained for varying concentration of the inhibitor and two substrate concentrations (30 and 90 μM). Abz-RS is a product of the substrate hydrolysis. Dependence of $1/v_0$ and k_a values for Pln and dependence of the $1/v$ values for Tln on Phin concentration were used for calculation of inhibition constants. The values are presented as a mean ± standard error.

conditions of high excess of inhibitor *versus* enzyme (in our experiments Phin concentration was at least four orders of magnitude higher than the Pln concentration). Therefore, this mechanism could be considered as a mechanism of induced fit – conformational adaptation of the enzyme to inhibitor or *vice versa* [47].

Hence, Phin, similar to M4in, is a slow-binding competitive inhibitor of Pln, but inhibits this enzyme significantly weaker. It was also found that Phin interacts with Pln according to the two-step mechanism, unlike M4in, which acts according to one-step mechanism with slow formation of the enzyme–inhibitor complex [7]. However, differences in the mechanisms are most likely associated with the different reaction conditions used in the experiments, which are determined by crucial differences in the binding efficiency.

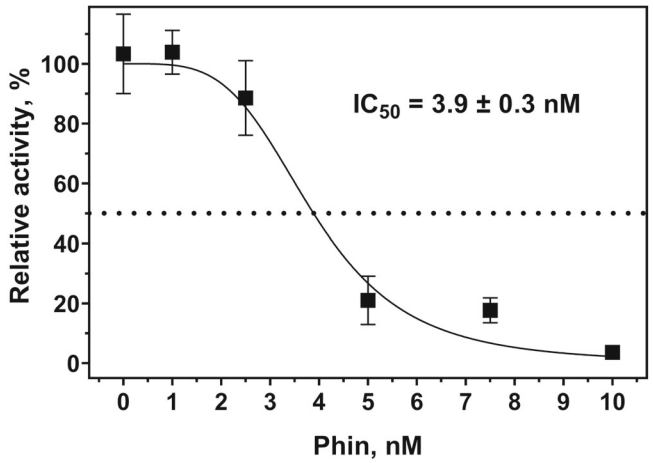

Fig. 6. Inhibition of activity of *P. laumondii* subsp. *laumondii* TT01 culture fluid by photorin (Phin). IC_{50}, half-maximal inhibitory concentration.

Kinetic curves describing interactions of Phin with Tln looked slightly curved (Fig. 5, Tln + Phin). At the same time, they are poorly approximated by the integrated reaction rate equation for slowly binding inhibitors [39], but are described well by the linear regression model ($R^2 > 0.98$). That is why in this case K_i was calculated according to the Dixon method for classic mechanism of inhibition (Table 3).

Thus, Phin is a classical inhibitor of Tln, which, likely, is determined by the structural differences in the active sites of Tln and Pln [48] – two enzymes belonging to one structural family of peptidases, but not by the structural differences of inhibitors. Unfortunately, currently there are no data on mechanism of Tln inhibition by emfourin.

Ability of culture fluid of *P. laumondii* to hydrolyze Abz-RSVIK(Dnp) is inhibited by photorin. Culture fluid of *P. laumondii* subsp. *laumondii* TT01 after 24 h of growth exhibits significant activity towards the Abz-RSVIK(Dnp) substrate [~4000 μmol/(min·ml)]. This activity is effectively suppressed by Phin, half-maximal inhibitory concentration IC_{50} is 3.9 ± 0.3 nM (Fig. 6).

DISCUSSION

In this study we obtained for the first time the data allowing to suggest that the protease S from *P. laumondii* subsp. *laumondii* TT01 (TT01) has a specific inhibitor – photorin. Phin is a second characterized inhibitor from the family I104 (according to classification of the MEROPS database). Comparison of Phin with another known representative of this family, its prototype emfourin (M4in), demonstrates that these two proteins differ significantly. Their sequences have only a quarter

of identical and around half of similar amino acid residues, which explains the differences in their secondary structure observed with the help of CD. Structural differences entail the differences in the processes of protein melting and, which is more important, differences in their inhibitory capacity.

The inhibitory action of Phin was investigated with respect to Pln and Tln, metalloproteases from different evolutionary groups of the M4 family (according to MEROPS classification). It was revealed that the mechanism of inhibition of Pln by photorin is different from the case of M4in, and inhibition constants are by 3 (K_i^*) and 4 (K_i) orders of magnitude higher (K_i for M4in is 52 pM [7]). This result does not seem unexpected, because Pln is a natural target of M4in, and Phin should be optimized for interaction with PrtS. Efficient suppression of hydrolysis of the peptide substrate of the protealysin-like proteases [37] by the culture fluid of TT01, the main protease of which is PrtS [49] supports suggestion of such optimization. Half-maximal inhibitory concentration (IC_{50}) in this case is in the nanomolar range, i.e., approximately 40-fold lower than the K_i^* observed in the case of Phin affecting Pln activity. The activity of Tln, which is not PLP, unlike Pln and PrtS [50], is suppressed by Phin even by one order of magnitude less than the activity of Pln (Table 3). Therefore, comparison of the available data on the inhibitory capacity of Phin and M4in indicates an evolutionary adaptation of the inhibitors of the M104 family to their natural targets, PLPs, from the same organisms.

Considering association of Phin and PrtS, it should be emphasized that organization of their genes in *P. laumondii* is different from the organization of corresponding genes of the inhibitor and protease in *S. proteamaculans*. In this bacterium the genes *pln* and *m4in*, as mentioned above, form a bicistronic operon, where the stop codon of the protease gene overlaps with the start codon of the inhibitor gene indicating translational coupling [7]. In the case of the genes *prtS* and *phin*, analysis of the TT01 genome sequence shows that in the intergenic region with the length of 160 bp there is a promoter in front of the inhibitor gene. Hence, in the case of *P. laumondii*, protease and inhibitor are encoded by the autonomous genes located one after another, which indicates differential regulation of transcription of these genes.

Differences in regulation of expression of the protease–inhibitor pair of genes likely are associated with the differences in their functions, which the proteins encoded by these genes have in different bacteria. Independent control at the transcription level allows flexibility in the control of the ELI/PLP ratio in the cell, while integration of the genes in one operon with translation coupling provides the possibility to fix this parameter. Taking into consideration probable multifunctionality of PLPs, it could be suggested that the independent regulation is required for realization of some functions of these proteases, but is excessive for others. In particular, decrease of the ELI/PLP ratio, which requires independent regulation, could be, for example, a trigger of an attack on the host immune system. And in the case when inhibitor plays a role of antitoxin in the system of interbacterial competition, it is sufficient that its concentration in the cell would be proportional to the protease concentration. On the other hand, independent regulation allows realization of both variants, and, in general, obviously, has high potential. In this context, independent regulation of genes likely emerges together with the increase of functions of the ELI/PLP pair.

Presence of Phin in the culture fluid, unlike in the case of M4in found only intracellularly, also implies possible differences in the functions of these inhibitors. The action of Phin, present extracellularly, could be associated with regulation of the PrtS activity in the medium. At the same time, other enzymes could also be targets of Phin. These could include thermolysin-like proteases produced by the competing microorganisms, or protease of the host organism. Hence, it cannot be ruled out that Phin has biological functions not associated with the activity of PrtS.

It must be mentioned in conclusion that the pair Phin and PrtS in the bacteria of *Photorhabdus* genus could be a very promising model for investigation of fundamental principles of proteolysis regulation. However, these studies should be preceded by investigation of the functions of these proteins in *Photorhabdus* and by the detailed characterization of interactions between Phin and PrtS.

Contributions. I.V.D. – concept and supervision of the study; I.M.B., A.O.S., K.N.Ch., M.A.K., A.M.V., V.V.F., S.Y.K. – conducting experiments; I.M.B., A.O.S., S.V.K., I.V.D. – discussion of the results of the study; I.M.B., A.O.S., I.V.D. – writing the paper; I.M.B., A.O.S., K.N.Ch., M.A.K., A.M.V., V.V.F., S.Y.K., S.V.K., I.V.D. – editing of the paper.

Funding. This study was financially supported by the Russian Science Foundation, grant no. 22-24-00135.

Acknowledgments. Equipment of the Center of Cellular and Genetic Technologies, Institute of Molecular Genetics, National Research Centre "Kurchatov Institute", was used in this work. The authors are grateful to D. I. Levitsky (Bach Institute of Biochemistry, Research Center of Biotechnology, Russian Academy of Sciences) for help in conducting experiments with differential scanning calorimetry.

Ethics declarations. The authors declare no conflict of interest in financial or any other sphere. All applicable international, national, and/or institutional guidelines for the care and use of animals were followed.

REFERENCES

1. Cabral-Pacheco, G. A., Garza-Veloz, I., Castruita-De la Rosa, C., Ramirez-Acuna, J. M., Perez-Romero, B. A., Guerrero-Rodriguez, J. F., Martinez-Avila, N., and Martinez-Fierro, M. L. (2020) The roles of matrix metalloproteinases and their inhibitors in human diseases, *Int. J. Mol. Sci.*, **21**, 9739, doi: 10.3390/ijms21249739.
2. D'Acunto, E., Fra, A., Visentin, C., Manno, M., Ricagno, S., Galliciotti, G., and Miranda, E. (2021) Neuroserpin: structure, function, physiology and pathology, *Cell. Mol. Life Sci.*, **78**, 6409-6430, doi: 10.1007/s00018-021-03907-6.
3. Kelly-Robinson, G. A., Reihill, J. A., Lundy, F. T., McGarvey, L. P., Lockhart, J. C., Litherland, G. J., Thornbury, K. D., and Martin, S. L. (2021) The serpin superfamily and their role in the regulation and dysfunction of serine protease activity in COPD and other chronic lung diseases, *Int. J. Mol. Sci.*, **22**, 6351, doi: 10.3390/ijms22126351.
4. Sillen, M., and Declerck, P. J. (2021) A narrative review on plasminogen activator inhibitor-1 and its (patho) physiological role: to target or not to target? *Int. J. Mol. Sci.*, **22**, 2721, doi: 10.3390/ijms22052721.
5. Wilkinson, D. J. (2021) Serpins in cartilage and osteoarthritis: what do we know? *Biochem. Soc. Trans.*, **49**, 1013-1026, doi: 10.1042/BST20201231.
6. Rawlings, N. D., Barrett, A. J., Thomas, P. D., Huang, X., Bateman, A., and Finn, R. D. (2018) The MEROPS database of proteolytic enzymes, their substrates and inhibitors in 2017 and a comparison with peptidases in the PANTHER database, *Nucleic Acids Res.*, **46**, D624-D632, doi: 10.1093/nar/gkx1134.
7. Chukhontseva, K. N., Berdyshev, I. M., Safina, D. R., Karaseva, M. A., Bozin, T. N., Salnikov, V. V., Konarev, P. V., Volkov, V. V., Grishin, A. V., Kozlovskiy, V. I., Kostrov, S. V., and Demidyuk, I. V. (2021) The protealysin operon encodes emfourin, a prototype of a novel family of protein metalloprotease inhibitors, *Int. J. Biol. Macromol.*, **169**, 583-596, doi: 10.1016/j.ijbiomac.2020.12.170.
8. Demidyuk, I. V., Gromova, T. Y., and Kostrov, S. V. (2013) *Protealysin*. in *Handbook of Proteolytic Enzymes* (Rawlings, N. D., and Salvesen, G., eds.), 3 Ed., Academic Press, Oxford, pp. 507-602.
9. Demidyuk, I. V., Kalashnikov, A. E., Gromova, T. Y., Gasanov, E. V., Safina, D. R., Zabolotskaya, M. V., Rudenskaya, G. N., and Kostrov, S. V. (2006) Cloning, sequencing, expression, and characterization of protealysin, a novel neutral proteinase from *Serratia proteamaculans* representing a new group of thermolysin-like proteases with short N-terminal region of precursor, *Protein Express. Purif.*, **47**, 551-561, doi: 10.1016/j.pep.2005.12.005.
10. Bozhokina, E. S., Tsaplina, O. A., Efremova, T. N., Kever, L. V., Demidyuk, I. V., Kostrov, S. V., Adam, T., Komissarchik, Y. Y., and Khaitlina, S. Y. (2011) Bacterial invasion of eukaryotic cells can be mediated by actin-hydrolysing metalloproteases grimelysin and protealysin, *Cell Biol. Int.*, **35**, 111-118, doi: 10.1042/CBI20100314.
11. Tsaplina, O. A., Demidyuk, I., Artamonova, T., Khodorkovsky, M., and Khaitlina, S. (2020) Cleavage of the outer membrane protein OmpX by protealysin regulates *Serratia proteamaculans* invasion, *FEBS Lett.*, **594**, 3095-3107, doi: 10.1002/1873-3468.13897.
12. Tsaplina, O. A., Efremova, T., Demidyuk, I., and Khaitlina, S. (2012) Filamentous actin is a substrate for protealysin, a metalloprotease of invasive *Serratia proteamaculans*, *FEBS J.*, **279**, 264-274, doi: 10.1111/j.1742-4658.2011.08420.x.
13. Tsaplina, O. A., Efremova, T. N., Kever, L. V., Komissarchik, Ya. Yu., Demidyuk, I. V., Kostrov, S. V., and Khaitlina, S. Y. (2009) Probing for actinase activity of protealysin, *Biochemistry (Moscow)*, **74**, 648-654, doi: 10.1134/s0006297909060091.
14. Khaitlina, S., Bozhokina, E., Tsaplina, O., and Efremova, T. (2020) Bacterial actin-specific endoproteases grimelysin and protealysin as virulence factors contributing to the invasive activities of Serratia, *Int. J. Mol. Sci.*, **21**, 4025, doi: 10.3390/ijms21114025.
15. Cabral, C. M., Cherqui, A., Pereira, A., and Simoes, N. (2004) Purification and characterization of two distinct metalloproteases secreted by the entomopathogenic bacterium *Photorhabdus* sp. Strain Az29, *Appl. Environ. Microbiol.*, **70**, 3831-3838, doi: 10.1128/aem.70.7.3831-3838.2004.
16. Held, K. G., LaRock, C. N., D'Argenio, D. A., Berg, C. A., and Collins, C. M. (2007) A metalloprotease secreted by the insect pathogen *Photorhabdus luminescens* induces melanization, *Appl. Environ. Microbiol.*, **73**, 7622-7628, doi: 10.1128/aem.01000-07.
17. Eshwar, A. K., Wolfrum, N., Stephan, R., Fanning, S., and Lehner, A. (2018) Interaction of matrix metalloproteinase-9 and Zpx in *Cronobacter turicensis* LMG 23827(T) mediated infections in the zebrafish model, *Cell. Microbiol.*, **20**, e12888, doi: 10.1111/cmi.12888.
18. Feng, T., Nyffenegger, C., Hojrup, P., Vidal-Melgosa, S., Yan, K. P., Fangel, J. U., Meyer, A. S., Kirpekar, F., Willats, W. G., and Mikkelsen, J. D. (2014) Characterization of an extensin-modifying metalloprotease: N-terminal processing and substrate cleavage pattern of *Pectobacterium carotovorum* Prt1, *Appl. Microbiol. Biotechnol.*, **98**, 10077-10089, doi: 10.1007/s00253-014-5877-2.
19. Kyöstiö, S. R., Cramer, C. L., and Lacy, G. H. (1991) Erwinia carotovora subsp. carotovora extracellular protease: characterization and nucleotide sequence of the gene, *J. Bacteriol.*, **173**, 6537-6546, doi: 10.1128/jb.173.20.6537-6546.1991.
20. Tsaplina, O., Khaitlina, S., Chukhontseva, K., Karaseva, M., Demidyuk, I., Bakhlanova, I., Baitin, D., Artamonova, T., Vedyaykin, A., Khodorkovskii, M., and Vishnyakov, I. (2022) Protealysin targets the bacterial housekeeping proteins FtsZ and RecA, *Int. J. Mol. Sci.*, **23**, 10787, doi: 10.3390/ijms231810787.

21. Clarke, D. J. (2008) *Photorhabdus*: a model for the analysis of pathogenicity and mutualism, *Cell. Microbiol.*, **10**, 2159-2167, doi: 10.1111/j.1462-5822.2008.01209.x.
22. Ciche, T. A., Kim, K. S., Kaufmann-Daszczuk, B., Nguyen, K. C., and Hall, D. H. (2008) Cell invasion and matricide during *Photorhabdus luminescens* transmission by heterorhabditis bacteriophora nematodes, *Appl. Environ. Microbiol.*, **74**, 2275-2287, doi: 10.1128/AEM.02646-07.
23. Cimen, H., Touray, M., Gulsen, S. H., Erincik, O., Wenski, S. L., Bode, H. B., Shapiro-Ilan, D., and Hazir, S. (2021) Antifungal activity of different *Xenorhabdus* and *Photorhabdus* species against various fungal phytopathogens and identification of the antifungal compounds from *X. szentirmaii*, *Appl. Microbiol. Biotechnol.*, **105**, 5517-5528, doi: 10.1007/s00253-021-11435-3.
24. Muangpat, P., Suwannaroj, M., Yimthin, T., Fukruksa, C., Sitthisak, S., Chantratita, N., Vitta, A., and Thanwisai, A. (2020) Antibacterial activity of *Xenorhabdus* and *Photorhabdus* isolated from entomopathogenic nematodes against antibiotic-resistant bacteria, *PLoS One*, **15**, e0234129, doi: 10.1371/journal.pone.0234129.
25. Bowen, D., Blackburn, M., Rocheleau, T., Grutzmacher, C., and ffrench-Constant, R. H. (2000) Secreted proteases from *Photorhabdus luminescens*: separation of the extracellular proteases from the insecticidal Tc toxin complexes, *Insect Biochem. Mol. Biol.*, **30**, 69-74, doi: 10.1016/s0965-1748(99)00098-3.
26. Marokházi, J., Kóczán, G., Hudecz, F., Gráf, L., Fodor, A., and Venekei, I. (2004) Enzymic characterization with progress curve analysis of a collagen peptidase from an enthomopathogenic bacterium, *Photorhabdus luminescens*, *Biochem. J.*, **379**, 633-640, doi: 10.1042/bj20031116.
27. Bradford, M. M. (1976) A rapid and sensitive method for the quantitation of microgram quantities of protein utilizing the principle of protein-dye binding, *Anal. Biochem.*, **72**, 248-254, doi: 10.1006/abio.1976.9999.
28. Gasparov, V. S., and Degtyar, V. G. (1994) Protein assay by the Coomassie brilliant blue G-250 dye binding method [in Russian], *Biokhmiya*, **59**, 763-777.
29. Laemmli, U. K. (1970) Cleavage of structural proteins during the assembly of the head of bacteriophage T4, *Nature*, **227**, 680-685, doi: 10.1038/227680a0.
30. Maniatis, T., Fritsch, E. F., Sambrook, J., and Engel, J. (1985) Molecular cloning – A laboratory manual, in *Acta Biotechnologica*, New York, Cold Spring Harbor Laboratory, **5**, 104-104, doi: 10.1016/0307-4412(83)90068-7.
31. Lennox, E. S. (1955) Transduction of linked genetic characters of the host by bacteriophage P1, *Virology*, **1**, 190-206, doi: 10.1016/0042-6822(55)90016-7.
32. Kozlovski, V., Brusov, V., Sulimenkov, I., Pikhtelev, A., and Dodonov, A. (2004) Novel experimental arrangement developed for direct fullerene analysis by electrospray time-of-flight mass spectrometry, *Rapid Commun. Mass Spectrom.*, **18**, 780-786, doi: 10.1002/rcm.1405.
33. Sreerama, N., and Woody, R. W. (2000) Estimation of protein secondary structure from circular dichroism spectra: comparison of CONTIN, SELCON, and CDSSTR methods with an expanded reference set, *Anal. Biochem.*, **287**, 252-260, doi: 10.1006/abio.2000.4880.
34. Drew, E. D., and Janes, R. W. (2020) PDBMD2CD: providing predicted protein circular dichroism spectra from multiple molecular dynamics-generated protein structures, *Nucleic Acids Res.*, **48**, W17-W24, doi: 10.1093/nar/gkaa296.
35. Chukhontseva, K. N., Salnikov, V. V., Morenkov, O. S., Kostrov, S. V., and Demidyuk, I. V. (2019) Protealysin is not secreted constitutively, *Protein Peptide Lett.*, **26**, 221-226, doi: 10.2174/0929866526666181212114907.
36. Schagger, H. (2006) Tricine-SDS-PAGE, *Nat. Protoc.*, **1**, 16-22, doi: 10.1038/nprot.2006.4.
37. Karaseva, M. A., Chukhontseva, K. N., Lemeskina, I. S., Pridatchenko, M. L., Kostrov, S. V., and Demidyuk, I. V. (2019) An internally quenched fluorescent peptide substrate for protealysin, *Sci. Rep.*, **9**, 14352, doi: 10.1038/s41598-019-50764-2.
38. Berdyshev, I. M., Karaseva, M. A., and Demidyuk, I. V. (2022) Assay for protealysin-like protease inhibitor activity, *Bio Protoc.*, **12**, e4528, doi: 10.21769/BioProtoc.4528.
39. Goliĉnik, M., and Stojan, J. (2004) Slow-binding inhibition: A theoretical and practical course for students, *Biochem. Mol. Biol. Educat.*, **32**, 228-235, doi: 10.1002/bmb.2004.494032040358.
40. Butterworth, P. J. (1972) The use of Dixon plots to study enzyme inhibition, *Biochim. Biophys Acta*, **289**, 251-253, doi: 10.1016/0005-2744(72)90074-5.
41. Dixon, M. (1953) The determination of enzyme inhibitor constants, *Biochem. J.*, **55**, 170-171, doi: 10.1042/bj0550170.
42. Bozin, T. N., Berdyshev, I. M., Chukhontseva, K. N., Karaseva, M. A., Konarev, P. V., Varizhuk, A. M., Lesovoy, D. M., Arseniev, A. S., Kostrov, S. V., Bocharov, E. V., and Demidyuk, I. V. (2023) NMR structure of emfourin, a novel protein metalloprotease inhibitor: insights into the mechanism of action, *J. Biol. Chem.*, **299**, 104585, doi: 10.1016/j.jbc.2023.104585.
43. Bozin, T. N., Chukhontseva, K. N., Lesovoy, D. M., Filatov, V. V., Kozlovskiy, V. I., Demidyuk, I. V., and Bocharov, E. V. (2021) NMR assignments and secondary structure distribution of emfourin, a novel proteinaceous protease inhibitor, *Biomol. NMR Assign.*, **15**, 361-366, doi: 10.1007/s12104-021-10030-x.
44. Chiu, M. H., and Prenner, E. J. (2011) Differential scanning calorimetry: An invaluable tool for a detailed thermodynamic characterization of macromolecules and their interactions, *J. Pharm. Bioallied Sci.*, **3**, 39-59, doi: 10.4103/0975-7406.76463.
45. Gianni, S., Dogan, J., and Jemth, P. (2014) Distinguishing induced fit from conformational selection, *Biophys. Chem.*, **189**, 33-39, doi: 10.1016/j.bpc.2014.03.003.
46. Hammes, G. G., Chang, Y. C., and Oas, T. G. (2009) Conformational selection or induced fit: a flux description

of reaction mechanism, *Proc. Natl. Acad. Sci. USA*, **106**, 13737-13741, doi: 10.1073/pnas.0907195106.

47. Masson, P., and Lushchekina, S. V. (2016) Slow-binding inhibition of cholinesterases, pharmacological and toxicological relevance, *Arch. Biochem. Biophys.*, **593**, 60-68, doi: 10.1016/j.abb.2016.02.010.
48. Demidyuk, I. V., Gromova, T. Y., Polyakov, K. M., Melik-Adamyan, W. R., Kuranova, I. P., and Kostrov, S. V. (2010) Crystal structure of the protealysin precursor: insights into propeptide function, *J. Biol. Chem.*, **285**, 2003-2013, doi: 10.1074/jbc.M109.015396.
49. Marokházi, J., Lengyel, K., Pekár, S., Felföldi, G., Patthy, A., Gráf, L., Fodor, A., and Venekei, I. (2004) Comparison of proteolytic activities produced by entomopathogenic *Photorhabdus* bacteria: strain- and phase-dependent heterogeneity in composition and activity of four enzymes, *Appl. Environ. Microbiol.*, **70**, 7311-7320, doi: 10.1128/aem.70.12.7311-7320.2004.
50. Demidyuk, I. V., Gasanov, E. V., Safina, D. R., and Kostrov, S. V. (2008) Structural organization of precursors of thermolysin-like proteinases, *Protein J.*, **27**, 343-354, doi: 10.1007/s10930-008-9143-2.